JOURNAL OF GUIDANCE, CONTROL, AND DYNAMICS
Vol. 30, No. 4, July–August 2007

Engineering Notes

ENGINEERING NOTES are short manuscripts describing new developments or important results of a preliminary nature. These Notes should not exceed 2500 words (where a figure or table counts as 200 words). Following informal review by the Editors, they may be published within a few months of the date of receipt. Style requirements are the same as for regular contributions (see inside back cover).

Solar Sail Formation Flying Around Displaced Solar Orbits

Shengping Gong,* Hexi Baoyin,† and Junfeng Li‡
Tsinghua University, 100084 Beijing, China

DOI: 10.2514/1.24315

Introduction

RECENTLY, attention has been focused on solar sail missions, such as the new artificial Lagrange points created by solar sails to be used to provide early warning of solar plasma storms, before they reach Earth [1,2]. There are several prior references with regard to such orbits in the literature. As early as 1929, Oberth mentioned in his study that solar radiation pressure would displace a reflector in an Earth polar orbit in the anti-sun direction, so that the orbit plane did not contain the center-of-mass of the Earth [3]. Later, in 1977, Austin et al. [4] noted that propulsive thrust can be used to displace the orbit of an artificial body, but only small displacements were considered for spacecraft proximity operations, and no analysis of the problem was provided. Similarly, Nock suggested a displaced orbit above Saturn's rings for in situ observation, however, again no analysis was given [3]. In 1981, Forward [5] considered a displaced solar sail north or south of the geostationary ring. However, because he did not use an active control, subsequent analysis has criticized this work and claimed that such orbits were impossible. More recently, McInnes and Simmons have done work in which large families of displaced orbits were found by considering the dynamics of a solar sail in a rotating frame [6], and the dynamics, stability, and control of different families of displaced orbits were investigated in detail [7,8]. Based on McInnes' and Simmons' work [6], Molostov and Shvartsburg considered a more realistic solar sail model with nonperfect reflectivity and discussed the effect of finite absorption of the sail on the displaced orbits [9,10]. However, studies of the relative motion of solar sails are rare in the literature. The original idea of formation flying around a displaced orbit considered in this note comes from the concept of combining a displaced orbit with formation flying to achieve greater resolution than a single sail for science missions.

This note outlines the characteristics of the relative motion around a displaced solar orbit and proposes some possible control strategies. Because the relative distance between the sails is very small compared with the distance from the sun to the sails, the relative equation of motion is linearized in the vicinity of a displaced solar orbit. Based on the linearized equation, two types of formations, seminatural and controlled formations, are discussed. The seminatural formations are performed with only sail attitude variations, but configurations of the relative orbits strongly depend on the orbit of the leader sail. Therefore, more complex controllers are adopted to build more sophisticated formations to meet special demands on the relative orbit configurations.

Displaced Solar Orbits

A displaced solar orbit [6–8] is a circular sun-centered orbit displaced above the ecliptic plane by directing a component of the solar radiation pressure force in a direction normal to the ecliptic. The sail orientation is defined by its normal vector $\boldsymbol{n}$, fixed in the rotating frame, and the sail performance is characterized by the sail lightness number β [5]. As shown in Fig. 1, to keep an equilibrium in the rotating frame, the sail pitch angle α and sail lightness number β for a displaced sun-centered orbit of radius ρ, displacement z, and orbital angular velocity ω are given by [11]

$$\tan\alpha = \frac{(z/\rho)(\omega/\tilde{\omega})^2}{(z/\rho)^2 + 1 - (\omega/\tilde{\omega})^2}, \qquad \tilde{\omega}^2 = \mu/r_1^3 \tag{1}$$

$$\beta = [1 + (z/\rho)^2]^{1/2}\frac{\{[1 + (z/\rho)^2] + [1 - (\omega/\tilde{\omega})^2]^2\}^{3/2}}{[(z/\rho)^2 + 1 - (\omega/\tilde{\omega})^2]^2} \tag{2}$$

where $r_1^2 = \rho^2 + z^2$.

Relative Motion

A two-sail formation is considered here in which the leader sail revolves on a displaced solar orbit and the follower is on a nearby orbit. The sails' state vectors are defined in terms of a set of Cartesian coordinates relative to the rotating frame. The origin of this frame is the mass center of the sun. In the rotating frame, the x axis is in the ecliptic plane and rotates around the sun with an angular velocity $\boldsymbol{\omega}$, the z axis is in the direction of the angular velocity, and the y axis forms a right-handed triad. Another rotating frame $o\xi\varsigma\eta$, labeled as the leader frame, has all its axes parallel to the axes of the rotating frame $Oxyz$ and has its origin at the mass center of the leader. In the frame $o\xi\varsigma\eta$, the position of the follower can be written as $\boldsymbol{\delta} = [x_2 - x_1 \quad y_2 - y_1 \quad z_2 - z_1]^T = [\xi \quad \varsigma \quad \eta]^T$, as shown in Fig. 1. The equations of motion of the sails in an inertial frame can then be written as

$$\ddot{\boldsymbol{r}}_1 = -f(\boldsymbol{r}_1) + g(\boldsymbol{r}_1, \boldsymbol{n}_1) \tag{3}$$

$$\ddot{\boldsymbol{r}}_2 = -f(\boldsymbol{r}_2) + g(\boldsymbol{r}_2, \boldsymbol{n}_2) \tag{4}$$

where $f(\boldsymbol{r}) = (\mu/r^3)\boldsymbol{r}$ is the solar gravitational force, $g(\boldsymbol{r}, \boldsymbol{n}) = \beta(\boldsymbol{n}\cdot\boldsymbol{r})^2(\mu/r^4)\boldsymbol{n}$ is the solar radiation pressure induced force, and μ is the solar gravitational constant. The relative equation of motion in the inertial frame is obtained by subtracting the two preceding equations

$$\ddot{\boldsymbol{\delta}} = \ddot{\boldsymbol{r}}_2 - \ddot{\boldsymbol{r}}_1 = f(\boldsymbol{r}_1) - f(\boldsymbol{r}_2) + g(\boldsymbol{r}_2, \boldsymbol{n}_2) - g(\boldsymbol{r}_1, \boldsymbol{n}_1) \tag{5}$$

The transformation of the acceleration between the inertial and rotational frames is given by

Received 28 March 2006; revision received 28 June 2006; accepted for publication 28 June 2006.

*Ph.D. Candidate, School of Aerospace; gsp04@mails.tsinghua.edu.cn.
†Assistant Professor, School of Aerospace; baoyin@tsinghua.edu.cn. Member AIAA.
‡Professor, School of Aerospace; lijunf@tsinghua.edu.cn.

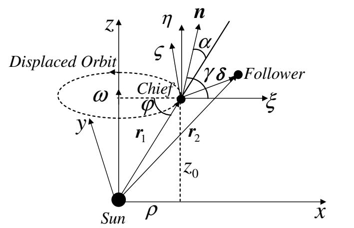

Fig. 1 Coordinates and angles definition.

$$\ddot{\boldsymbol{\delta}} = \frac{\mathrm{d}^2\boldsymbol{\delta}}{\mathrm{d}t^2} + 2\boldsymbol{\omega} \times \frac{\mathrm{d}\boldsymbol{\delta}}{\mathrm{d}t} + \boldsymbol{\omega} \times (\boldsymbol{\omega} \times \boldsymbol{\delta}) + \dot{\boldsymbol{\omega}} \times \boldsymbol{\delta} \tag{6}$$

where $\mathrm{d}/\mathrm{d}t$ denotes derivative with respect to the rotating frame. In our case, $\dot{\boldsymbol{\omega}} = 0$. Thus, the equation of relative motion in the rotating frame can be written as

$$\frac{\mathrm{d}^2\boldsymbol{\delta}}{\mathrm{d}t^2} + 2\boldsymbol{\omega} \times \frac{\mathrm{d}\boldsymbol{\delta}}{\mathrm{d}t} + \boldsymbol{\omega} \times (\boldsymbol{\omega} \times \boldsymbol{\delta}) = f(\boldsymbol{r}_1) - f(\boldsymbol{r}_2) + g(\boldsymbol{r}_2, \boldsymbol{n}_2) - g(\boldsymbol{r}_1, \boldsymbol{n}_1) \tag{7}$$

In formation flying, the relative distance between sails, $|\boldsymbol{r}_2 - \boldsymbol{r}_1|$, is usually very small compared with r_1 or r_2. Therefore, $f(\boldsymbol{r}_2)$ can be expanded around $\boldsymbol{r}_1$ and the first-order approximation can be given as

$$f(\boldsymbol{r}_2) = f(\boldsymbol{r}_1) + \left.\frac{\partial f}{\partial \boldsymbol{r}}\right|_{\boldsymbol{r}=\boldsymbol{r}_1} \boldsymbol{\delta} + o\left(\frac{\boldsymbol{\delta}}{r_1}\right) \tag{8}$$

where $\partial f/\partial \boldsymbol{r} = (\mu/r^3)I_{3\times 3} - (3\mu/r^5)\boldsymbol{r}\boldsymbol{r}^T$. To maintain the follower in the vicinity of the leader, the sail lightness numbers β_2 and β_1 should be very close, and so should the normal vectors, therefore $g(\boldsymbol{r}_2, \boldsymbol{n}_2, \beta_2)$ can be expanded around $(\boldsymbol{r}_1, \boldsymbol{n}_1, \beta_1)$

$$g(\boldsymbol{r}_2, \boldsymbol{n}_2, \beta_2) = g(\boldsymbol{r}_1, \boldsymbol{n}_1, \beta_1) + \left.\frac{\partial g}{\partial \boldsymbol{r}}\right|_{\substack{\boldsymbol{r}=\boldsymbol{r}_1\\ \boldsymbol{n}=\boldsymbol{n}_1\\ \beta=\beta_1}} \boldsymbol{\delta} + \left.\frac{\partial g}{\partial \boldsymbol{n}}\right|_{\substack{\boldsymbol{r}=\boldsymbol{r}_1\\ \boldsymbol{n}=\boldsymbol{n}_1\\ \beta=\beta_1}} (\boldsymbol{n}_2 - \boldsymbol{n}_1) + \left.\frac{\partial g}{\partial \beta}\right|_{\substack{\boldsymbol{r}=\boldsymbol{r}_1\\ \boldsymbol{n}=\boldsymbol{n}_1\\ \beta=\beta_1}} (\beta_2 - \beta_1) + o(\boldsymbol{n}_2 - \boldsymbol{n}_1) + o\left(\frac{\beta_2 - \beta_1}{\beta_1}\boldsymbol{n}_1\right) + o\left(\frac{\boldsymbol{\delta}}{r_1}\right) \tag{9}$$

where $\frac{\partial g}{\partial \boldsymbol{r}} = \frac{2\beta\mu(\boldsymbol{n}\cdot\boldsymbol{r})}{r^4}\boldsymbol{n}\boldsymbol{n}^T - \frac{4\beta\mu(\boldsymbol{n}\cdot\boldsymbol{r})^2}{r^6}\boldsymbol{n}\boldsymbol{r}^T$

$$\frac{\partial g}{\partial \boldsymbol{n}} = \frac{\beta\mu(\boldsymbol{n}\cdot\boldsymbol{r})^2}{r^4}I_{3\times 3} + \frac{2\beta\mu(\boldsymbol{n}\cdot\boldsymbol{r})}{r^4}\boldsymbol{n}\boldsymbol{r}^T$$

$$\frac{\partial g}{\partial \beta} = \frac{\mu(\boldsymbol{n}\cdot\boldsymbol{r})^2}{r^4}\boldsymbol{n}$$

Substituting Eqs. (8) and (9) into (7), the first-order approximation can be written as

$$\frac{\mathrm{d}^2\boldsymbol{\delta}}{\mathrm{d}t^2} + 2\boldsymbol{\omega} \times \frac{\mathrm{d}\boldsymbol{\delta}}{\mathrm{d}t} + \boldsymbol{\omega} \times (\boldsymbol{\omega} \times \boldsymbol{\delta}) - \left(\frac{2\beta_1\mu(\boldsymbol{n}_1\cdot\boldsymbol{r}_1)}{r_1^4}\boldsymbol{n}_1\boldsymbol{n}_1^T - \frac{4\beta_1\mu(\boldsymbol{n}_1\cdot\boldsymbol{r}_1)^2}{r_1^6}\boldsymbol{n}_1\boldsymbol{r}_1^T - \frac{\mu}{r_1^3}I_{3\times 3} + \frac{3\mu}{r_1^5}\boldsymbol{r}_1\boldsymbol{r}_1^T\right)\boldsymbol{\delta} - \left(\frac{\beta_1\mu(\boldsymbol{n}_1\cdot\boldsymbol{r}_1)^2}{r_1^4}I_{3\times 3} + \frac{2\beta_1\mu(\boldsymbol{n}_1\cdot\boldsymbol{r}_1)}{r_1^4}\boldsymbol{n}_1\boldsymbol{r}_1^T\right)(\boldsymbol{n}_2 - \boldsymbol{n}_1) - \frac{\mu(\boldsymbol{n}_1\cdot\boldsymbol{r}_1)^2}{r_1^4}\boldsymbol{n}_1(\beta_2 - \beta_1) = 0 \tag{10}$$

where $\boldsymbol{r}_1 = [\rho \quad 0 \quad z_0]^T$, $\boldsymbol{n}_1 = [\cos\gamma_1 \quad 0 \quad \sin\gamma_1]^T$, and γ is the sail elevation angle [7] measured from the ecliptic plane in the plane spanned by vectors $\boldsymbol{r}$ and $\boldsymbol{\omega}$, as shown in Fig. 1. The equation of relative motion can be rewritten as

$$\frac{\mathrm{d}^2\boldsymbol{\delta}}{\mathrm{d}t^2} + 2J\frac{\mathrm{d}\boldsymbol{\delta}}{\mathrm{d}t} + M\boldsymbol{\delta} = N\delta\boldsymbol{n} + P\delta\beta \tag{11}$$

where the coefficient matrices are

$$J = \begin{bmatrix} 0 & -\omega & 0 \\ \omega & 0 & 0 \\ 0 & 0 & 0 \end{bmatrix}$$

$$M = -\left(\frac{2\beta_1\mu(\boldsymbol{n}_1\cdot\boldsymbol{r}_1)}{r_1^4}\boldsymbol{n}_1\boldsymbol{n}_1^T - \frac{4\beta_1\mu(\boldsymbol{n}_1\cdot\boldsymbol{r}_1)^2}{r_1^6}\boldsymbol{n}_1\boldsymbol{r}_1^T - \frac{\mu}{r_1^3}I_{3\times 3} + \frac{3\mu}{r_1^5}\boldsymbol{r}_1\boldsymbol{r}_1^T\right)$$

$$N = \frac{\beta_1\mu(\boldsymbol{n}_1\cdot\boldsymbol{r}_1)^2}{r_1^4}I_{3\times 3} + \frac{2\beta_1\mu(\boldsymbol{n}_1\cdot\boldsymbol{r}_1)}{r_1^4}\boldsymbol{n}_1\boldsymbol{r}_1^T$$

$$P = \frac{\mu(\boldsymbol{n}_1\cdot\boldsymbol{r}_1)^2}{r_1^4}\boldsymbol{n}_1$$

For formation flying, attention is focused on the stable solutions of Eq. (11) but not asymptotically stable ones, because the follower sail will drift toward the leader and thus no formation is achieved for the asymptotically stable solutions. However, $\delta\boldsymbol{n}$ in Eq. (11) is independent of the relative distance $\boldsymbol{\delta}$, and it is difficult to carry out the stability analysis without any restriction on the variation $\delta\boldsymbol{n}$. In the subsequent analysis, we will give some restrictions on $\delta\boldsymbol{n}$ to implement several types of possible formation and control strategies.

Formations

Displaced solar orbits have been categorized into three types by McInnes and Simmons [6] labeled as type 1, $\omega = \tilde{\omega}$; type 2, $\omega =$ constant, one special case is $\omega = \omega_e$ (Earth-synchronous); and type 3, $\omega = \omega_o$ (ω_o is obtained by setting the derivative of β with respect to ω to zero in Eq. (2) to minimize β). In this note, the formations around type 1 and type 2 are studied. In this section, two types of formations, seminatural and controlled, are studied. For the seminatural formations, three cases $\delta\boldsymbol{n} = 0$, $\delta\gamma = 0$, and $\delta\alpha = 0$ with $\delta\beta = 0$ are considered to obtain simpler ones. The relative stability for seminatural formations is defined as the follower stays in the vicinity of the leader, and neither diverges from nor converges to it. The stability is determined by calculating the eigenvalues of the controlled system. If all the eigenvalues have nonpositive real part and at least one with zero real part, the relative motion is referred to as stable. For controlled formations, the sail attitude and lightness number vary continuously to track some desired reference relative orbits and thereby achieve more sophisticated formations.

Seminatural Formations

The first formation is obtained by taking $\delta\boldsymbol{n} = 0$. This guarantees that the normal vector of the follower sail is always the same as that of the leader, which is assumed to be a constant vector in the rotating frame. Then, the relative linearized equation of motion can be written as

$$\frac{\mathrm{d}^2\boldsymbol{\delta}}{\mathrm{d}t^2} + 2J\frac{\mathrm{d}\boldsymbol{\delta}}{\mathrm{d}t} + M\boldsymbol{\delta} = 0 \tag{12}$$

For the formation around type 1 displaced orbits, it can be analytically proven that all relative motions are unstable (hereafter, all the detailed procedures of the proofs are omitted). For the formation around type 2, the expression becomes too complicated to obtain an analytical solution for the stable regions. Here, the stable region of the Earth-synchronous family is numerically determined and shown as the shadowed region in Fig. 2 where one can see that a stable relative orbit can be obtained within only a small range of parameters.

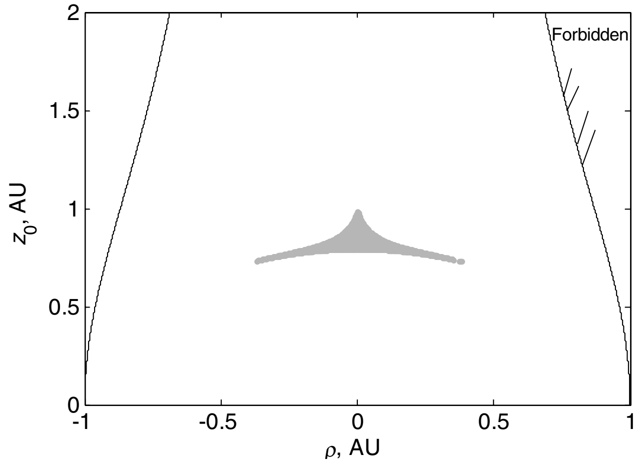

Fig. 2 Stable region of the Earth-synchronous family of orbits.

The second formation is determined by taking $\delta\gamma = 0$. This means that the elevation angle of the follower sail is fixed in the plane spanned by vectors $\boldsymbol{r}_2$ and $\boldsymbol{\omega}$. Then, the normal of the follower sail can be written as

$$\boldsymbol{n} = \left[\cos\gamma_1 \frac{x_2}{\sqrt{x_2^2+y_2^2}} \quad \cos\gamma_1 \frac{y_2}{\sqrt{x_2^2+y_2^2}} \quad \sin\gamma_1\right]^T \tag{13}$$

where x_2, y_2, and z_2 are Cartesian of the follower in the coordinates shown in Fig. 1. Thus, the variation of the normal vector can be approximated in the position feedback form by linearizing $\boldsymbol{n}_2$ around $\boldsymbol{n}_1$, given by

$$\delta\boldsymbol{n} = \boldsymbol{n}_2 - \boldsymbol{n}_1 = \left.\frac{\partial \boldsymbol{n}}{\partial \boldsymbol{r}}\right|_{r_1} \qquad \boldsymbol{\delta} = \begin{bmatrix} 0 & 0 & 0 \\ 0 & \cos\gamma_1 \frac{1}{\rho} & 0 \\ 0 & 0 & 0 \end{bmatrix} \boldsymbol{\delta} \tag{14}$$

Substituting Eq. (14) into Eq. (11), it can be analytically proven again that in this case the formations around type 1 are unstable, and the stable region of the Earth-synchronous family of formations around type 2 are numerically found to be the same as the results of Fig. 4 found in [7].

The third formation is defined by taking $\delta\alpha = 0$. This means that the pitch angle α of the follower sail is fixed in the plane spanned by vectors $\boldsymbol{r}_2$ and $\boldsymbol{\omega}$. The normal of the follower sail can then be given as

$$\boldsymbol{n} = \left[\cos(\alpha_1 + \varphi_2)\frac{x_2}{\sqrt{x_2^2+y_2^2}} \quad \cos(\alpha_1 + \varphi_2)\frac{y_2}{\sqrt{x_2^2+y_2^2}} \quad \sin(\alpha_1 + \varphi_2)\right]^T \tag{15}$$

where

$$\varphi_2 = \tan^{-1}\frac{z_2}{\sqrt{x_2^2 + y_2^2}}$$

Thus, the variation of the normal vector can be approximated in position feedback form by linearizing $\boldsymbol{n}_2$ around $\boldsymbol{n}_1$, given as

$$\delta\boldsymbol{n} = \boldsymbol{n}_2 - \boldsymbol{n}_1 = \left.\frac{\partial \boldsymbol{n}}{\partial \boldsymbol{r}}\right|_{r_1}$$
$$\boldsymbol{\delta} = \begin{bmatrix} \frac{\sin\varphi_1 \sin\gamma_1}{r_1} & 0 & -\frac{\cos\varphi_1 \sin\gamma_1}{r_1} \\ 0 & \frac{\cos\gamma_1}{\rho} & 0 \\ -\frac{\sin\varphi_1 \cos\gamma_1}{r_1} & 0 & \frac{\cos\varphi_1 \cos\gamma_1}{r_1} \end{bmatrix} \boldsymbol{\delta} \tag{16}$$

Similarly, substituting Eq. (16) into Eq. (11), it can be analytically proven that formations around type 1 are always stable. Again, the stability of formations around type 2 in the Earth-synchronous family is numerically determined to be stable in all possible regions. Later formations are very attractive for mission application because a large stable region exists and no complicated feedback control is required.

As aforementioned, a stable region exists in all formations around type 2 in the Earth-synchronous family, but the relative motion around a given displaced orbit, which is completely determined by the initial relative states and leader's orbit, cannot be designed arbitrarily. The relative orbits around the given Earth-synchronous displaced orbits for each case with the given initial values are shown in Fig. 3 in which the motion is shown in the rotating frame for 10 years.

Controlled Formations

As explained in the preceding section, the seminatural controllers are not able to control formations in certain relative configurations. To achieve a desired relative configuration, more complex control laws are needed to be put forward. Such laws are probably not a desirable option at present because the sail attitude is required to vary continuously. Here, we will consider two kinds of control schemes to obtain the desired formations.

In the first controlled formation, we adjust two attitude angles and the sail lightness number to control the relative orbit. To determine the normal vector of sail, θ and ϕ are adopted, where θ is the angle between the normal and the xz plane, and ϕ is the angle between the x-axis and the projection of the normal in the xz plane. Then, the normal vector of the sail can be given by

$$\boldsymbol{n} = \left[\cos\theta\cos\phi \quad \sin\theta \quad \cos\theta\sin\phi\right]^T \tag{17}$$

The control variables are defined by $\boldsymbol{u} = [\delta\phi \quad \delta\theta \quad \delta\beta]^T$,

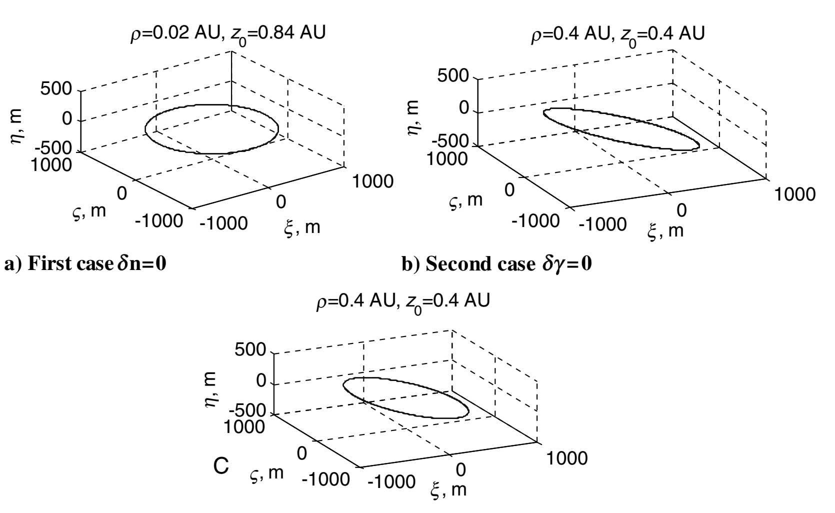

a) First case δn=0
b) Second case $\delta\gamma$=0
c) Third case $\delta\alpha$=0

Fig. 3 Seminatural formations.

$\delta\phi = \phi_2 - \phi_1$, $\delta\theta = \theta_2 - \theta_1 = \theta_2$, and $\delta\beta = \beta_2 - \beta_1$. To maintain the follower sail in the vicinity of the displaced solar orbit, $\delta\phi$ and $\delta\theta$ should be small. Therefore, $\boldsymbol{n}_2$ can be expanded around (ϕ_1, θ_1) and first-order approximation can be obtained as

$$\delta\boldsymbol{n} = \boldsymbol{n}_2 - \boldsymbol{n}_1 = \frac{\partial\boldsymbol{n}}{\partial(\phi,\theta)}\bigg|_{(\phi_1,\theta_1)}\begin{bmatrix}\delta\phi\\ \delta\theta\end{bmatrix} = \begin{bmatrix}-\sin\phi_1 & 0\\ 0 & 1\\ \cos\phi_1 & 0\end{bmatrix}\begin{bmatrix}\delta\phi\\ \delta\theta\end{bmatrix} \tag{18}$$

The controlled relative equation of motion is obtained by substituting Eq. (18) into Eq. (11), yielding

$$\frac{\mathrm{d}^2\boldsymbol{\delta}}{\mathrm{d}t^2} + 2J\frac{\mathrm{d}\boldsymbol{\delta}}{\mathrm{d}t} + M\boldsymbol{\delta} = B\boldsymbol{u} \tag{19}$$

The coefficient matrix is given by

$$B = [N\tfrac{\partial\boldsymbol{n}}{\partial(\phi,\theta)}|_{(\phi_1,\theta_1)} \quad P]$$

The first-order system is given by

$$\dot{X}_r = AX_r + \begin{bmatrix}\mathbf{0}\\ B\end{bmatrix}u \tag{20}$$

where $X_r = [\boldsymbol{\delta}^T \quad \dot{\boldsymbol{\delta}}^T]^T$. It can be proven that the system is controllable. The linear solution is obtained from the linearized dynamics of the nonlinear relative system in the neighborhood of the displaced solar orbit. Consider the general quadratic cost function for a linear quadratic regulator (LQR)

$$J = \frac{1}{2}\int_0^\infty [(X_r - X_{\mathrm{ref}})^T Q(X_r - X_{\mathrm{ref}}) + u^T Ru]\,\mathrm{d}t \tag{21}$$

where the matrices Q and R represent the weight of the state errors and the control input, respectively, both of which are symmetric positive definite. Therefore, what is required is to find a linear state feedback by solving a Riccati matrix algebraic equation to get

$$u = -K(X_r - X_{\mathrm{ref}}) \tag{22}$$

where X_{ref} is the reference relative orbit.

The second controlled formation uses the same control variables as the first controller. Input feedback linearization (IFL) is employed to control the formation. In our case, it is a partial nonlinear strategy instead of a complete one, because the control force is linearized. The equation of motion can be written as

$$\frac{\mathrm{d}^2\boldsymbol{\delta}}{\mathrm{d}t^2} + 2\boldsymbol{\omega}\times\frac{\mathrm{d}\boldsymbol{\delta}}{\mathrm{d}t} + \boldsymbol{\omega}\times(\boldsymbol{\omega}\times\boldsymbol{\delta}) = f(\boldsymbol{r}_1) - f(\boldsymbol{r}_2) + \frac{\partial g}{\partial\boldsymbol{r}}\bigg|_{\substack{r=r_1\\ n=n_1\\ \beta=\beta_1}}\boldsymbol{\delta} + \boldsymbol{f}_u \tag{23}$$

Equation (23) can be rewritten as

$$\frac{\mathrm{d}^2\boldsymbol{\delta}}{\mathrm{d}t^2} = h(\boldsymbol{\delta},\dot{\boldsymbol{\delta}}) + \boldsymbol{f}_u \tag{24}$$

where

$$h(\boldsymbol{\delta},\dot{\boldsymbol{\delta}}) = -\left[2\boldsymbol{\omega}\times\frac{\mathrm{d}\boldsymbol{\delta}}{\mathrm{d}t} + \boldsymbol{\omega}\times(\boldsymbol{\omega}\times\boldsymbol{\delta}) - f(\boldsymbol{r}_1) + f(\boldsymbol{r}_2) - \frac{\partial g}{\partial\boldsymbol{r}}\bigg|_{\substack{r=r_1\\ n=n_1\\ \beta=\beta_1}}\boldsymbol{\delta}\right]$$

and $\boldsymbol{f}_u$ is the control input. In input feedback linearization, the control $\boldsymbol{f}_u$ is selected such that

$$\boldsymbol{f}_u = -h(\boldsymbol{\delta},\dot{\boldsymbol{\delta}}) + \upsilon(\boldsymbol{\delta},\dot{\boldsymbol{\delta}},\ddot{\boldsymbol{\delta}}) \tag{25}$$

The control acceleration $\upsilon(\boldsymbol{\delta},\dot{\boldsymbol{\delta}},\ddot{\boldsymbol{\delta}})$ in Eq. (25) is designed to be representative of the desired nominal motion $\boldsymbol{\delta}_{\mathrm{ref}}$. For a critically damped response

$$\upsilon = \ddot{\boldsymbol{\delta}}_{\mathrm{ref}} - 2\lambda(\dot{\boldsymbol{\delta}} - \dot{\boldsymbol{\delta}}_{\mathrm{ref}}) - \lambda^2(\boldsymbol{\delta} - \boldsymbol{\delta}_{\mathrm{ref}}) \tag{26}$$

Therefore, the control vector is given by

$$u = B^{-1}\boldsymbol{f}_u \tag{27}$$

Numerical Simulation

In the following example, the integrations are based on the complete nonlinear equation of relative motion (7). The leader is on an Earth-synchronous displaced solar orbit of $\rho = 0.98$ AU and $z_0 = 4\times 10^5$ km. The reference relative orbit of the follower sail is a 10 km-radius circular orbit in the $\xi\varsigma$ plane, and centered at the leader. The period of the relative motion, which can be selected at will, is 1%

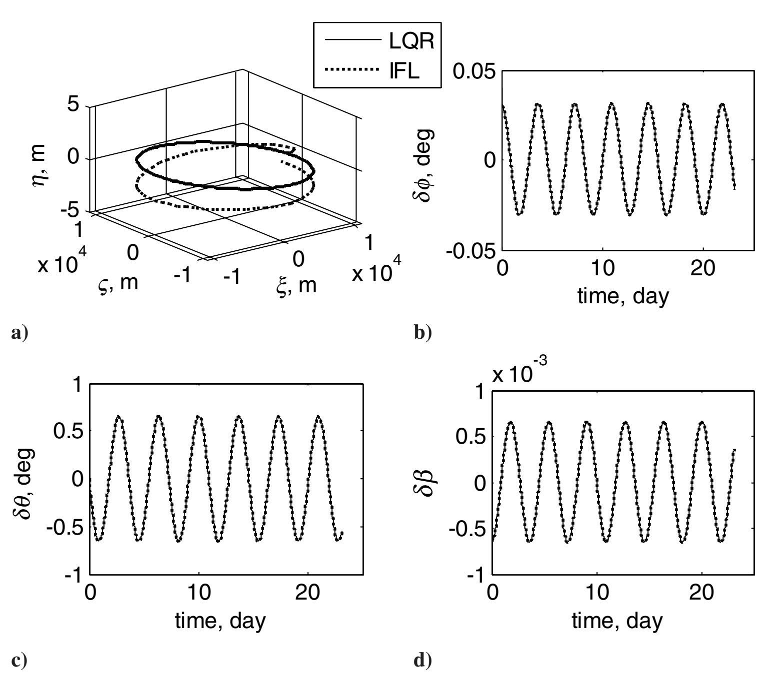

Fig. 4 Controlled formations.

of Earth's orbital period in the simulation. The follower is assumed to be on the reference orbit at the initial time. We set $Q = I_{6\times6}$ and $R = 1 \times 10^6 I_{3\times3}$ for LQR, the simulation results are shown in Fig. 4, where Fig. 4a illustrates the relative orbit and Figs. 4b–4d show the control input. According to the time history of the control variables, the formation requires a maximum control angle variation of less than 1 deg and a sail lightness number variation of less than 0.001, so that the validity of the linearization can be guaranteed. The results in the figures reflect that the two controllers obtain similar results except for the initial time.

Conclusions

This note outlines solar sail relative motion around displaced orbits, with the relative equations of motion linearized in the vicinity of a displaced solar orbit. Based on those equations, three seminatural formations are studied in some detail. One formation among them is very attractive for practical applications because of its simplicity and large stable regions. However, the formation configurations of the seminatural formations depend too strongly on the leader's orbit. To improve the adaptability of the formation to special missions, two controlled formations are proposed to achieve certain relative configurations as designed. All the formations are validated by simulations, which are based on the full nonlinear equations of the system.

Acknowledgment

The authors would like to acknowledge John Lewis, University of Arizona, for many helpful discussions and meticulous revision for the note.

References

[1] West, J. L., "NOAA/DOD/NASA Geostorm Warning Mission," Jet Propulsion Lab, California Inst. of Technology," JPL D-13986, Pasadena, CA, Oct. 1996.

[2] Prado, J. Y., Perret, A., Pignolet, G., and Dandouras, I., "Using a Solar Sail for a Plasma Storm Early Warning System," International Academy of Astronautics, Paper 96-IAA. 3.3.06, Oct. 1996.

[3] McInnes, C. R., "Dynamics, Stability and Control of Non-Keplerian Orbits," Ph.D. Dissertation, Univ. of Glasgow, 2002.

[4] Austin, R. E., Dod, R. E., and Terwilliger, C. H., "Ubiquitous Solar Electric Propulsion Stage," *Acta Astronautica*, Vol. 4, 1977, pp. 671–694.

[5] Forward, R. L., "Light-Levitated Geostationary Cylindrical Orbits," *Journal of the Astronautical Sciences*, Vol. 29, No. 1, 1981, pp. 73–80.

[6] McInnes, C. R., and Simmons, F. L., "Solar Sail Halo Orbits 1: Heliocentric Case," *Journal of Spacecraft and Rockets*, Vol. 29, No. 4, 1992, pp. 466–471.

[7] McInnes, C. R., "Passive Control of Displaced Solar Sail Orbits," *Journal of Guidance, Control, and Dynamics*, Vol. 21, No. 6, 1998, pp. 975–982.

[8] McInnes, C. R., and Macpherson, K. P., "Solar Sail Halo Trajectories: Dynamics and Applications," *42nd International Astronautical Congress*, International Astronautical Federation Paper IAF-91-334, Oct. 1991.

[9] Molostov, A. A., and Shvartsburg, A. A., "Heliocentric Halos for a Solar Sail with Absorption," *Soviet Physics, Doklady*, Vol. 37, No. 3, 1992, pp. 149–152.

[10] Molostov, A. A., and Shvartsburg, A. A., "Heliocentric Synchronous Halos for a Solar Sail with Absorption," *Soviet Physics, Doklady*, Vol. 37, No. 4, 1992, pp. 195–197.

[11] McInnes, C. R., "Solar Sail Mission Applications for Non-Keplerian Orbits," *Acta Astronautica*, Vol. 45, Nos. 4–9, 1999, pp. 567–575.